Available online at www.sciencedirect.com

ScienceDirect

Energy Procedia 77 (2015) 619 – 625

Energy Procedia

5th International Conference on Silicon Photovoltaics, SiliconPV 2015

Effects of solar cell processing steps on dislocation luminescence in multicrystalline silicon

Hieu T. Nguyen[a,*], Fiacre E. Rougieux[a], Fan Wang[b], and Daniel Macdonald[a]

[a]*Research School of Engineering, College of Engineering and Computer Science, The Australian National University, Canberra, ACT 2601, Australia*

[b]*Department of Electronic Materials Engineering, Research School of Physics and Engineering, The Australian National University, Canberra, ACT 2601, Australia*

Abstract

We examine the impacts of hydrogenation and phosphorus gettering steps on the deep-level photoluminescence spectra of dislocations and the surrounding regions in multicrystalline silicon wafers, using micro-photoluminescence spectroscopy with micron-scale spatial resolution. We found that the D1 line, originating from secondary defects around dislocation sites, was enhanced significantly after gettering but remained unchanged after hydrogenation, suggesting that the former process reduced the concentration of metal impurities around the dislocations while the latter process did not alter the relevant properties of defects and impurities. In addition, the D3 and D4 intensities were found to be unchanged after different processing steps, indicating that the intrinsic structure of the dislocations was not affected by the investigated processes. Finally, we report empirical evidence supporting the hypothesis that D3 is not the phonon replica of D4 due to their different intensity ratio at different locations in the wafers.

Peer review by the scientific conference committee of SiliconPV 2015 under responsibility of PSE AG

Keywords: Crystalline silicon; deep level; dislocations; grain boundaries; photoluminescence (PL); photovoltaic cells

* Corresponding author.
E-mail address: hieu.nguyen@anu.edu.au

Peer review by the scientific conference committee of SiliconPV 2015 under responsibility of PSE AG
doi:10.1016/j.egypro.2015.07.089

1. Introduction

Recently, there has been an increasing interest in employing spectrally-resolved photoluminescence (PL) as an accurate and non-destructive characterization tool in silicon photovoltaics. By capturing the luminescence signal emitted from transitions of free carriers between the two band edges of crystalline silicon, fundamental properties of this material have been determined such as the band-to-band (BB) absorption coefficient [1-3], radiative recombination coefficient [2,4,5], temperature dependence of the band gap [6], and the extent of band-gap narrowing in heavily-doped silicon [7,8]. Also, BB spectral PL has been employed to extract the minority carrier diffusion length in silicon wafers [9,10] and bricks [11], to quantify light trapping in plasmonic structures [12], to investigate the effects of different surface morphologies [13,14] as well as carrier profiles [14] on the spectrum shapes, and recently to study properties of thin heavily-doped layers of cell pre-cursors [15]. On the other hand, defects and impurities occupying energy states within the forbidden gap of crystalline silicon can give rise to deep-level luminescence spectra, with the peak energies lower than that of the BB peak. These deep-level spectra contain distinct signatures for different kinds of defects and impurities such as Cr-B pairs [16], oxygen precipitates [17], Fe precipitates [18], and dislocations [19,20] in crystalline silicon.

In multicrystalline silicon (mc-Si), dislocation networks are one of the key factors limiting the final cell efficiency [21], and usually occur at small angle grain boundaries (SAGBs) and other sub-grain boundaries (sub-GBs). These dislocation sites have been reported to emit four distinct deep-level lines, known as D1, D2, D3, and D4. The doublet D1/D2 originates from secondary defects and impurities decorated around dislocations [22,23], whereas the doublet D3/D4 reflects the intrinsic properties of dislocations [22-26]. These results have been confirmed recently by Tajima *et al.* [23], in which D1 and D2 were found to occur around SAGBs, and D3 and D4 were present directly on SAGBs. Recently, utilizing the micron-scale spatial resolution of a confocal microscope PL spectroscopy system, we have shown that the D1 intensity was enhanced when the dislocations were cleaned of metal impurities after gettering, whereas the D2 intensity still remained the same, and confirmed that D1 and D2 had different origins [27]. Also, we proposed that D3 was not the phonon replica of D4 due to their different energy shifting when moving away from the sub-GBs.

Since the D lines reflect the properties of dislocations and the surrounding local conditions, they can be employed as a tool to monitor the behavior of defects and impurities around dislocations and the dislocations themselves during cell fabrication processes. Moreover, phosphorous gettering and hydrogenation are two essential steps which are naturally incorporated during the formation of diffused layers, and of antireflection coating (ARC) layers by chemical vapor deposition (CVD) and their subsequent firing. Thus, an insightful understanding of the behaviors of the D lines after these two processing steps may provide more information about the impact of gettering and hydrogenation on dislocations. Therefore, in this work, utilizing the high spatial resolution of a micro-PL (μPL) spectroscopy system, we report findings regarding the various effectiveness of the gettering process along the sub-GBs based on the D line emissions, and also investigate the behaviors of the D lines after the hydrogenation process. In addition, we also report further experimental findings to support the hypothesis that D3 is not the phonon replica of D4 [27].

2. Experimental details

The experimental setup in this study is described in detail elsewhere [27]. The μPL spectroscopy system has a spatial resolution of about 3 microns and a spectral resolution of about 0.25 nm. The sample temperature was kept constant at 79 K using a liquid-nitrogen-cooled cryostat. The samples studied here are directionally solidified, boron-doped p-type mc-Si wafers having a background doping of about 9×10^{15} cm^{-3}. Three samples were cut from three consecutive wafers in the same ingot, and chemically etched with an etchant of HF and HNO_3 to remove saw damage and to achieve optically polished surfaces. After that, the first sample was kept in the as-cut state. The second sample was passivated with a layer of SiN_x:H deposited by plasma-enhanced chemical vapor deposition (PECVD) using ammonia and silane as precursor gases. It was then annealed at 700 ^oC for 30 minutes in a N_2 gas environment in a quartz tube furnace to distribute hydrogen throughout the sample thickness. The third sample went through an extended phosphorous gettering process [28], which is described in greater details in Ref. 27. The sheet resistance of the resultant diffused layer was about 30 Ω/□. All samples were chemically etched again to remove

residual layers left after the previous processing steps, leaving bare silicon surfaces. Finally, they were immersed in a defect etchant consisting of acetic/nitric/hydrofluoric acids for 16 hours [29,30]. The purpose of this etching step is to delineate the sub-GBs, which are otherwise not observable under the optical microscope. The final thickness of these samples is around 250 microns.

3. Results and analysis

First, we examine the behaviors of D1 and D2 after the hydrogenation and gettering steps. In order to ensure that the presence of the D3 and D4 lines does not affect our analysis on the D1 and D2 lines, the investigated sub-GB was chosen to have strong D1 and D2 emissions, but low D3 and D4 emissions. We captured the PL spectra at a location about 10 microns away from the same sub-GB for the three samples. Each individual spectrum was then decomposed with 5 Gaussian peaks representing the four lines D1, D2, D3, D4, and the first phonon replica of the band-to-band line (BBPR). The amplitudes of these Gaussian peaks are the intensities of their corresponding PL lines. Here we did not fit the band-to-band (BB) peak with the Gaussian function since this BB peak was distinctly sharp at 79 K [2,3], allowing us to isolate the BB peak. We note that decomposing the spectrum in this way is necessary to accurately estimate the intensities of the individual D lines, since there is significant overlap between them. By contrast, a common way to investigate their spatial distributions, in particular D1 and D2, is to apply band-pass filters to collect individual components of the spectra. However, the detected PL signal using band-pass filters is, in principle, still the aggregate signal of multiple components. For example, in Fig. 1c, the apparent intensity of D2 is almost as twice the intensity of the decomposed D2 peak, since the D2 line in this case occurs on the tail of the more intense D1 peak. This effect may give a misleading conclusion regarding the change of the D2 line if applying band-pass filters.

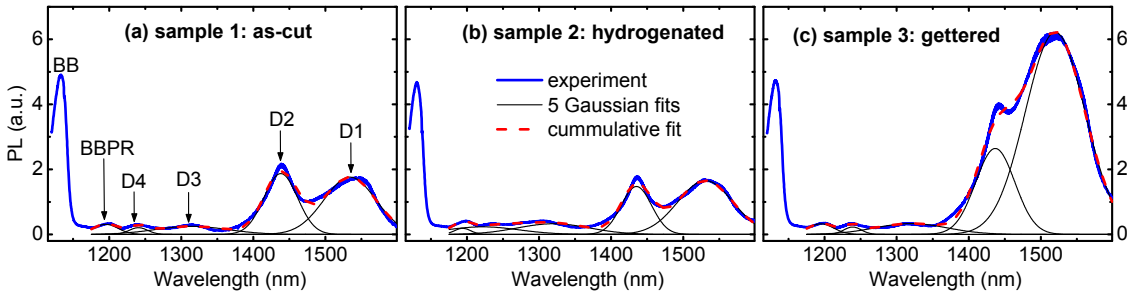

Fig. 1. Comparison of PL spectra among (a) as-cut, (b) hydrogenated, and (c) gettered samples at a location about 10 microns away from the same sub-GB at 79 K.

In Fig. 1, the spectrum of the hydrogenated sample is similar to that of the as-cut sample, whereas the spectrum of the gettered sample changes significantly. Since the D1 and D2 lines are emitted by the secondary defects or impurities trapped by the strain field around the dislocation sites, the consistency of the D1 and D2 intensities indicates that the hydrogenation process performed in this study is not effective in altering or passivating these defects and impurities around the dislocations. However, after gettering, D1 is enhanced notably whereas D2 does not change significantly. This behavior of D1 has been reported by our group recently, and was suggested as being due to a reduction in the concentration of metal impurities, in particular Fe, around the sub-GBs after gettering [27]. This finding can be compared with the results from Johnston *et al.* [31], in which the authors found an enhancement of the sub-band gap luminescence from defect clusters in mc-Si wafers after the phosphorus diffusion, although via the imaging technique employing a long-pass filter (> 1350 nm). Due to this behavior of D1, we therefore hypothesize that the D1 line originates from only the secondary defects, and the metal impurities may form complexes with the D1 centers, thus alternating their energy levels and suppressing their luminescence efficiency. Moreover, as we performed line scans parallel to this sub-GB at a distance about 10 microns away from the sub-GB, the spectra of the as-cut sample are almost the same, whereas those of the gettered sample are altered significantly, as plotted in Fig. 2. The D1 intensity increases from the starting point to the final point of the line scan on the

gettered sample. We continued performing the line scans again but in the opposite direction, and observed the opposite trend of the D1 intensities, indicating that the observed increment of D1 is not due to scanning artifacts. Therefore, the results in Fig. 2 suggest that the gettering extent of metal impurities varies along the length of the sub-GB itself. The more effective the gettering process is, the higher the D1 intensity is.

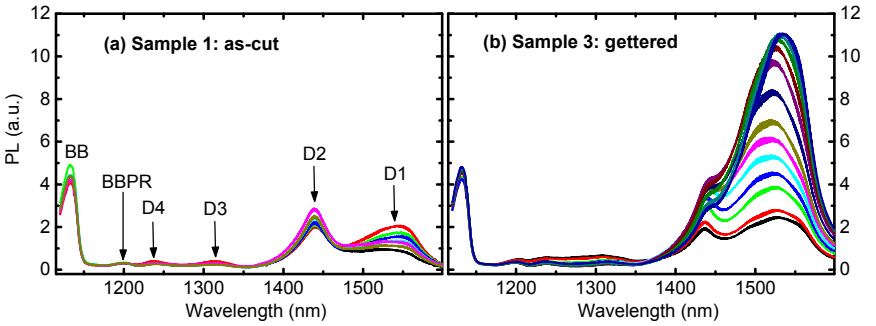

Fig. 2. PL spectra from line scans parallel to the sub-GB of (a) as-cut and (b) gettered samples. The line scans were performed at a distance about 10 microns away from the sub-GB, and each spectrum in the figure corresponds to one position along the line scans.

In order to avoid the differences in local conditions, as shown above, from affecting our general conclusions, we performed 80-micron line scans parallel to this sub-GB in 5-micron step sizes, at different distances (5, 10, and 15 microns) away from this sub-GB. Fig. 3 shows the average intensities of the D1, D2, and BB peaks (after the total spectrum was decomposed), along with one standard deviation error bars. As can be readily seen in Figs. 3a and 3b, the D1 intensity of the gettered sample is notably higher than that of the other two samples, although the BB intensity in Fig. 3c is the same among the three samples. Also, the extent of the D1 error bars of the gettered sample is consistently much larger than that of the other two samples at different distances. Therefore, we conclude that the hydrogenation process used in our study does not affect the D1 and D2 luminescence efficiencies, whereas the gettering process enhances the deep-level luminescence of D1 due to the reduction of metal impurities, and this effect varies along the sub-GB itself.

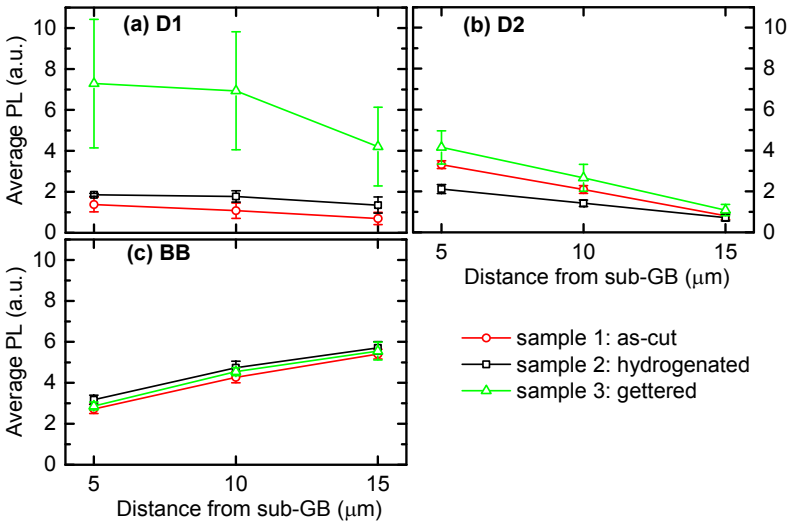

Fig. 3. Average PL intensities, along with one standard deviation error bars, of (a) D1, (b) D2, and (c) BB peaks among the three samples at 79 K.

Next, we investigated the behaviors of D3 and D4 after the two processing steps. For this we chose sub-GBs having strong D3 and D4 emissions. The D3 and D4 intensities are consistent among the as-cut, hydrogenated, and gettered samples for the investigated sub-GBs as shown in Fig. 4. Since D3 and D4 are thought to reflect the intrinsic properties of the dislocation sites [22-27], this consistency suggests that the structure of dislocations is very stable and not altered after different processing steps including hydrogenation, gettering, and the high thermal treatment incorporated during the gettering process. This behavior of D3 and D4 is similar to the results in Ref. 27, in which the D3 and D4 lines were found to be unchanged after gettering, high temperature annealing, and Fe implantation steps. Note that the D1 intensity after gettering (Fig. 4c) is increased as twice that of the as-cut sample (Fig. 4a), whereas the D2 intensity remains the same.

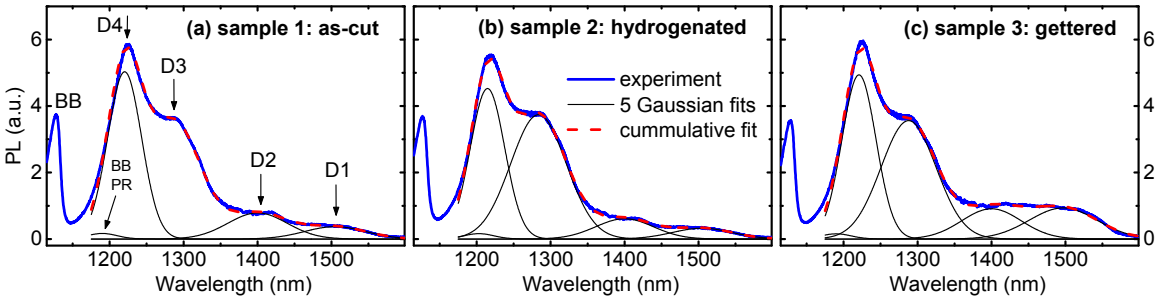

Fig. 4. Comparison of PL spectra among (a) as-cut, (b) hydrogenated, and (c) gettered samples on the same sub-GB at 79 K.

Finally, as can be qualitatively seen from Fig. 5a, the intensity ratio between D3 and D4 varies significantly from location to location. Note that although the D1 and D2 intensities are very strong at location 01, the high energy side of the D2 Gaussian peak is not overlapping with the center of the D3 peak when decomposing the spectrum as shown in Fig. 5b, and hence the D3 peak intensity is not affected by the high energy side of the D2 distribution. Therefore, the intensity ratio between D3 and D4 is not affected by D1 and D2 emissions in Fig. 4a. This different behavior between D3 and D4 contradicts the common belief that D3 is the phonon replica of D4 [23,25], but is similar to what was reported in Ref. 27, in which the peak energy was shifted differently between D3 and D4. If D3 is a phonon replica of D4, their intensity ratio should be the same at a certain temperature regardless of the locations. Therefore, we conclude that D3 is not the phonon replica of D4.

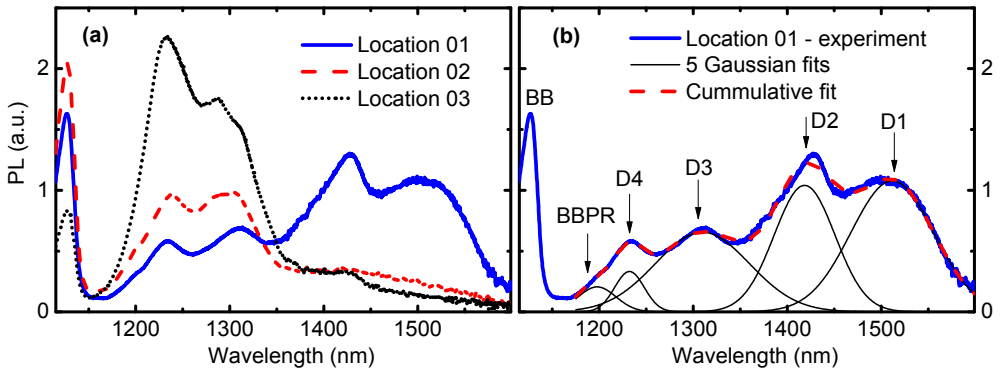

Fig. 5. (a) PL spectra of the as-cut sample at different locations at 79 K. (b) Gaussian fits of PL spectrum at location 01 on the as-cut sample at 79 K.

4. Conclusion

We have empirically examined the impacts of hydrogenation and gettering steps on the deep-level photoluminescence spectra from dislocations. Our results suggest that the reduced concentration of metal impurities trapped around the dislocation sites after gettering enhances the luminescence of D1, while hydrogenation has no effect on the intensity of D1. The effectiveness of the gettering is found to vary along the sub-grain boundaries due to the different enhancement of the D1 intensity. In addition, the structure of the dislocations is found not to be affected by the two processes due to the consistency of the D3 and D4 intensities. Finally, we have reported the difference in intensity ratio between D3 and D4, suggesting that D3 is not the phonon replica of D4.

Acknowledgements

This work has been supported by the Australian Research Council (ARC) and the Australian Renewable Energy Agency (ARENA) through research grant RND009. The Australian National Fabrication Facility is acknowledged for providing access to some of the facilities used in this work. The authors are in debt to Prof. H. Tan for providing access to the spectroscopic equipment.

References

[1] E. Daub and P. Würfel, Ultralow values of the absorption coefficient of Si obtained from luminescence, Phys. Rev. Lett. 74, 1020 (1995).
[2] T. Trupke, M. A. Green, P. Würfel, P. P. Altermatt, A. Wang, J. Zhao, and R. Corkish, Temperature dependence of the radiative recombination coefficient of intrinsic crystalline silicon, J. Appl. Phys. 94, 4930 (2003).
[3] H. T. Nguyen, F. E. Rougieux, B. Mitchell, and D. Macdonald, Temperature dependence of the band-band absorption coefficient in crystalline silicon from photoluminescence, J. Appl. Phys. 115, 043710 (2014).
[4] P. P. Altermatt, F. Geelhaar, T. Trupke, X. Dai, A. Neisser, and E. Daub, Injection dependence of spontaneous radiative recombination in crystalline silicon: Experimental verification and theoretical analysis, Appl. Phys. Lett. 88, 261901 (2006).
[5] H. T. Nguyen, S. C. Baker-Finch, and D. Macdonald, Temperature dependence of the radiative recombination coefficient in crystalline silicon from spectral photoluminescence, Appl. Phys. Lett. 104, 112105 (2014).
[6] W. Bludau, A. Onton, and W. Heinke, Temperature dependence of the band gap of silicon, J. Appl. Phys. 45, 1846 (1974).
[7] J. Wagner, Photoluminescence and excitation spectroscopy in heavily doped n- and p-type silicon, Phys. Rev. B 29, 2002 (1984).
[8] J. Wagner, Band-gap narrowing in heavily doped silicon at 20 and 300 K studied by photoluminescence, Phys. Rev. B 32, 1323 (1985).
[9] P. Würfel, T. Trupke, T. Puzzer, E. Schäffer, W. Warta, and S. W. Glunz, Diffusion lengths of silicon solar cells from luminescence images, J. Appl. Phys. 101, 123110 (2007).
[10] J. A. Giesecke, M. Kasemann, M. C. Schubert, P. Würfel, and W. Warta, Separation of local bulk and surface recombination in crystalline silicon from luminescence reabsorption, Progress in Photovoltaics: Res. & Appl. 18, 10 (2011).
[11] B. Mitchell, M. K. Juhl, M. A. Green, and T. Trupke, Full spectrum photoluminescence lifetime analyses on silicon bricks, IEEE Journal of Photovoltaics 3, 962 (2013).
[12] C. Barugkin, Y. Wan, D. Macdonald, and K. R. Catchpole, Evaluating plasmonic light trapping with photoluminescence, IEEE Journal of Photovoltaics 3, 1292 (2013).
[13] C. Schinke, D. Hinken, J. Schmidt, K. Bothe, and R. Brendel, Modeling the spectral luminescence emission of silicon solar cells and wafers, IEEE Journal of Photovoltaics 3, 1038 (2013).
[14] H. T. Nguyen, F. E. Rougieux, S. C. Baker-Finch, and D. Macdonald, Impact of carrier profile and rear-side reflection on photoluminescence spectra in planar crystalline silicon wafers at different temperatures, IEEE Journal of Photovoltaics 5, 77 (2015).
[15] H. T. Nguyen, D. Yan, F. Wang, P. Zheng, Y. Han, and D. Macdonald, Micro-photoluminescence spectroscopy on heavily-doped layers of silicon solar cells, Physica Status Solidi: Rapid Research Letters 9, 230 (2015).
[16] H. Conzelmann and J. Weber, Photoluminescence from chromium-boron pair in silicon, Physica B+C 116, 291 (1983).
[17] S. Binetti, S. Pizzini, E. Leoni, R. Somaschini, A. Castaldini, and A. Cavallini, Optical properties of oxygen precipitates and dislocations in silicon, J. Appl. Phys. 92, 2437 (2002).
[18] P. Gundel, M. C. Schubert, W. Kwapil, J. Schön, M. Reiche, H. Savin, M. Yli-Koski, J. A. Sans, G. Martinez-Criado, W. Seifert, W. Warta, and E. R. Weber, Micro-photoluminescence spectroscopy on metal precipitates in silicon, Physica Status Solidi: Rapid Research Letters 3, 230 (2009).
[19] R. Sauer, J. Weber, J. Stolz, E. R. Weber, K.-H. Küsters, and H. Alexander, Dislocation-related photoluminescence in silicon, Applied Physics A 36, 1 (1985).
[20] M. Tajima, Spectroscopy and topography of deep-level luminescence in photovoltaic silicon, IEEE Journal of Photovoltaics 4, 1452 (2014).
[21] B. Sopori, P. Rupnowski, V. Mehta, V. Budhraja, S. Johnston, N. Call, H. Mountinho, M. Al-Jassim, A. Shaikh, M. Seacrist, and D. Carlson, Performance limitations of mc-si solar cells caused by defect clusters, ECS Transactions 18, 1049 (2009).

[22] H. Sugimoto, M. Inoue, M. Tajima, A. Ogura, and Y. Ohshita, Analysis of intra-grain defects in multicrystalline silicon wafers by photoluminescence mapping and spectroscopy, Japanese Journal of Applied Physics 45, L641 (2006).
[23] M. Tajima, Y. Iwata, F. Okayama, H. Toyota, H. Onodera, and T. Sekiguchi, Deep-level photoluminescence due to dislocations and oxygen precipitates in multicrystalline Si, J. Appl. Phys. 111, 113523 (2012).
[24] T. Sekiguchi and K. Sumino, Cathodoluminescence study on dislocations in silicon, J. Appl. Phys. 79, 3253 (1996).
[25] Tz. Arguirov, W. Seifert, M. Kittler, and J. Reif, Temperature behaviour of extended defects in solar grade silicon investigated by photoluminescence and EBIC, Mater. Sci. Eng. B 102, 251 (2003).
[26] W. Lee, J. Chen, B. Chen, J. Chang, and T. Sekiguchi, Cathodoluminescence study of dislocation-related luminescence from small-angle grain boundaries in multicrystalline silicon, Applied Physics Letters 94, 112103 (2009).
[27] H. T. Nguyen, F. E. Rougieux, F. Wang, H. Tan, and D. Macdonald, Micrometer-scale deep-level spectral photoluminescence from dislocations in multicrystalline silicon, IEEE Journal of Photovoltaics 5, 799 (2015).
[28] S. P. Phang and D. Macdonald, Direct comparison of boron, phosphorus, and aluminum gettering of iron in crystalline silicon, J. Appl. Phys. 109, 073521 (2011).
[29] W.C. Dash, Copper precipitation on dislocations in silicon, J. Appl. Phys 27, 1193 (1956).
[30] Y. Kashigawa, R. Shimokawa, and M. Yamanaka, Highly sensitive etchants for delineation of defects in single- and polycrystalline silicon materials, J. Electrochem. Soc. 143, 4079 (1996).
[31] S. Johnston, H. Guthrey, F. Yan, K. Zaunbrecher, M. Al-Jassim, P. Rakotoniaina, and M. Kaes, Correlating multicrystalline silicon defect types using photoluminescence, defect-band emission, and lock-in thermography imaging techniques, IEEE Journal of Photovoltaics 4, 348 (2014).